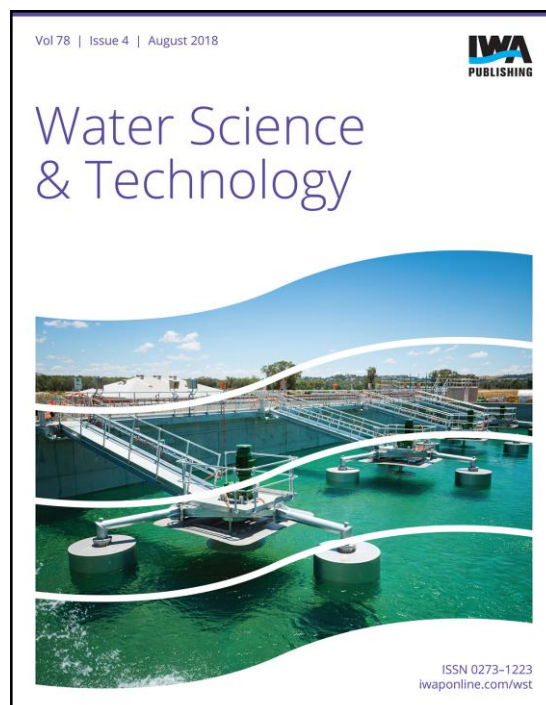


ELECTRONIC OFFPRINT

Use of this pdf is subject to the terms described below



This paper was originally published by IWA Publishing. The author's right to reuse and post their work published by IWA Publishing is defined by IWA Publishing's copyright policy.

If the copyright has been transferred to IWA Publishing, the publisher recognizes the retention of the right by the author(s) to photocopy or make single electronic copies of the paper for their own personal use, including for their own classroom use, or the personal use of colleagues, provided the copies are not offered for sale and are not distributed in a systematic way outside of their employing institution. **Please note that you are not permitted to post the IWA Publishing PDF version of your paper on your own website or your institution's website or repository.**

If the paper has been published "Open Access", the terms of its use and distribution are defined by the Creative Commons licence selected by the author.

Full details can be found here: <http://iwaponline.com/content/rights-permissions>

Please direct any queries regarding use or permissions to wst@iwap.co.uk

Greenhouse gas emissions from membrane bioreactors: analysis of a two-year survey on different MBR configurations

Giorgio Mannina, Kartik Chandran, Marco Capodici, Alida Cosenza, Daniele Di Trapani and Mark C. M. van Loosdrecht

ABSTRACT

This study aimed at evaluating the nitrous oxide (N₂O) emissions from membrane bioreactors (MBRs) for wastewater treatment. The study investigated the N₂O emissions considering multiple influential factors over a two-year period: (i) different MBR based process configurations; (ii) wastewater composition (municipal or industrial); (iii) operational conditions (i.e. sludge retention time, carbon-to-nitrogen ratio, C/N, hydraulic retention time); (iv) membrane modules. Among the overall analysed configurations, the highest N₂O emission occurred from the aerated reactors. The treatment of industrial wastewater, contaminated with salt and hydrocarbons, provided the highest N₂O emission factor (EF): 16% of the influent nitrogen for the denitrification/nitrification-MBR plant. The lowest N₂O emission (EF = 0.5% of the influent nitrogen) was obtained in the biological phosphorus removing bed-MBR plant likely due to an improvement in biological performances exerted by the co-presence of both suspended and attached biomass. The influent C/N ratio has been identified as a key factor affecting the N₂O production. Indeed, a decrease of the C/N ratio (from 10 to 2) promoted the increase of N₂O emissions in both gaseous and dissolved phases, mainly related to a decreased efficiency of the denitrification processes.

Key words | global warming, MBR, nitrous oxide emission, wastewater treatment

Giorgio Mannina (corresponding author)
Marco Capodici

Alida Cosenza

Daniele Di Trapani

Dipartimento di Ingegneria Civile, Ambientale,
Aerospaziale, dei Materiali,
Università degli Studi di Palermo,
Viale delle Scienze, Ed. 8, 90128,
Palermo,
Italy
E-mail: giorgio.mannina@unipa.it

Giorgio Mannina

Kartik Chandran

Department of Earth and Environmental
Engineering,
Columbia University,
500 West 120th Street,
New York, NY 10027,
USA

Mark C. M. van Loosdrecht

Department of Biotechnology,
Delft University of Technology,
Van der Maasweg 9, 2629 HZ,
Delft,
The Netherlands

INTRODUCTION

During the last decade, the awareness that wastewater treatment plants (WWTPs) are responsible for greenhouse gas emissions (GHGs) has considerably increased as evident from the large number of research papers published on the topic in the last 10 years (Kampschreur *et al.* 2009; Ahn *et al.* 2010; Stenström *et al.* 2014; Ni & Yuan 2015; Mannina *et al.* 2017a). Among the emitted GHGs from WWTPs, N₂O has been identified of having the major interest. Despite the amount of N₂O emitted from WWTPs is considerably lower than CO₂ or CH₄, the major interest on its emission from WWTPs is due to its high global warming potential (GWP), 298 times higher than that of CO₂ for a 100-year time scale (IPCC 2007). Several studies have been performed with the aim to better understand the core pathways of N₂O formation (Kampschreur *et al.* 2009; Yu & Chandran 2010; Yu *et al.* 2010; Chandran *et al.* 2011; Law *et al.* 2012; Wunderlin *et al.* 2012; Yu *et al.* 2018), most of the studies reported in

literature are related to conventional activated sludge systems (CASs). The acquired knowledge may not be transferred into innovative systems such as membrane bioreactors (MBRs). On the other hand, MBR systems have attracted increasing attention in the last few years, due to several advantages compared to conventional processes (Di Trapani *et al.* 2011a, 2011b). More specifically, MBR systems provide high effluent quality, small footprint and moderate sludge production rates compared to CAS (Stephenson *et al.* 2000).

The specific peculiarities of MBRs (biomass selection; absence of secondary clarifier which can contribute in N₂O production; intensive aeration for fouling mitigation in membrane compartment which can promote N₂O stripping, etc.) may hamper a direct transferability of the results derived for CAS systems (Nuansawan *et al.* 2016). Therefore, there is an imperative need to increase the knowledge on N₂O emission from MBRs, through ad-hoc

experimental and mathematical modelling activities, since only a few studies have been reported so far (Mannina et al. 2016a, 2016b).

The main goal of this study is to investigate GHG production/emission from MBRs, referring in particular to N_2O . A detailed investigation where the occurring N transformations are discussed is available in the literature (Mannina et al. 2016a, 2016b; Mannina 2017; Mannina et al. 2017a, 2017b, 2018). Here, different pilot plant configurations, wastewater characteristics and operational conditions have been analysed in a two-year experimental survey (PRIN2012 2012). The goal was to build-up a wide experimental database related to the MBR with the final aim to gain insights and allow, as a further step, the application of mathematical models.

MATERIAL AND METHODS

Four different pilot plants were investigated during the experimental period (namely, SB-MBR, DN-MBR, UCT-MBR and UCT-IFAS-MBR) (Figure 1). The pilot plants were equipped with specific funnel shape covers that guaranteed gas accumulation in the headspace, to capture the produced gas by sampling. The experimental period had a duration of almost two years and was aimed at investigating the influence of operational variables (SRT, C/N ratio and HRT-SRT), influent features (municipal and industrial wastewater) on N_2O production and emission (Mannina et al. 2017a, 2017b).

Briefly, pilot plant N.1, referred to as SB-MBR, was designed according to a pre-denitrification scheme and was operated in a sequential feeding mode. It consisted of two in-series reactors: one anoxic (volume: 45 L volume) and one aerobic (volume: 224 L), followed by an MBR compartment (volume: 50 L). The experimental campaign was divided into six phases, each characterized by a different salt concentration in the feeding wastewater. In detail, the salt concentration was gradually increased from 0 to 10 g $NaCl L^{-1}$ (Phase I: no salt addition; Phase II: 2 g $NaCl L^{-1}$; Phase III: 4 g $NaCl L^{-1}$; Phase IV: 6 g $NaCl L^{-1}$; Phase V: 8 g $NaCl L^{-1}$; Phase VI: 10 g $NaCl L^{-1}$). This campaign was aimed at assessing the system response in terms of N_2O production when subjected to salt increase in the feeding wastewater, also evaluating the biomass acclimation to a gradual salinity increase in the feeding wastewater. This experimental period was also propaedeutic to the experimental period carried out on pilot plant N.2 (see below), for the treatment of industrial wastewater characterized by the simultaneous presence of salt and hydrocarbons (ship-board slops).

Pilot plant N.2, referred to as DN-MBR, consisted of the same reactors described in pilot plant N.1 with the difference that influent flow rate was fed in continuous mode to the pilot plant. The experimental gathering campaign had a duration of 90 days and was divided in two phases, characterized by different features of the inlet wastewater. In detail, Phase I was characterized by an increasing salinity of the influent (from 10 g $NaCl L^{-1}$ up to 20 g $NaCl L^{-1}$), while

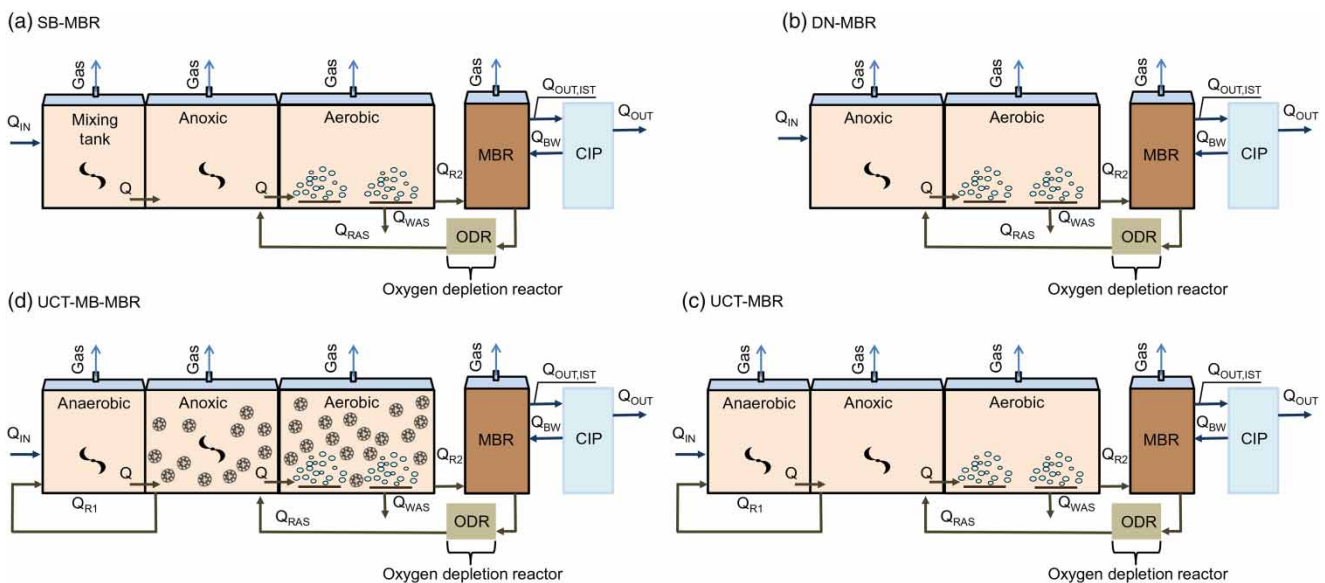


Figure 1 | Schematic layout of the investigated pilot plants: SB-MBR (a), pre-denitrification MBR (b), UCT-MBR (c) and UCT-MB-MBR (d).

in Phase II, the inlet wastewater was characterized by constant salinity (20 g NaCl L⁻¹) and hydrocarbons dosage (Mannina 2017).

Pilot plant N.3, referred to as UCT-MBR, was characterized by one anaerobic (volume: 62 L), one anoxic (volume: 102 L), and one aerobic (volume: 211 L) in-series reactors, according to the University of Cape Town (UCT) scheme (Ekama *et al.* 1983). The UCT-MBR pilot plant was fed with a mixture of real and synthetic wastewater, the latter characterized by sodium acetate, glycerol, di-potassium hydrogen phosphate and ammonium chloride. The experimental campaign was divided in two phases, each characterized by a different value of the inlet C/N ratio. Phase I, C/N of 10 (duration: 41 days), Phase II, C/N of 5 (duration: 39 days).

Pilot plant N.4, referred to as IFAS-UCT-MBR, was characterized by one anaerobic (volume: 62 L), one anoxic (volume: 102 L), and one aerobic (volume: 211 L) in-series reactors, according to the UCT scheme (Ekama *et al.* 1983). The pilot plant was realized according to the integrated fixed-film activated sludge (IFAS) moving bed biofilm reactor (MBBR) based MBR configuration, with the presence of both activated sludge and biofilm. The suspended plastic carriers for biofilm growth have been added to the anoxic and the aerobic reactors, with filling fraction of 15 and 40%, corresponding to specific area of 75 and 200 m² m⁻³, respectively. The experimental campaign has a duration of 340 days and was aimed at investigating the influence of operational variables (namely, SRT, C/N ratio and HRT-SRT) on N₂O production and emission. The pilot plant was fed with a mixture of real and synthetic wastewater, in order to meet the desired C/N value of the inlet wastewater.

Furthermore, it has to be stressed that in pilot plants N.1 and N.2 the solid-liquid separation was achieved by means of hollow fiber ultrafiltration (UF) module Zenon Zeeweed, ZW 10 (specific area of the filtration module equal to 0.98 m² and nominal porosity equal to 0.04 μm). Conversely, pilot plants N.3 and N.4 were equipped with the UF module Koch PURON® 3 bundle with specific area equal to 1.40 m² and nominal porosity of 0.03 μm.

Further details on pilot plants description, as well as on experimental campaigns, the reader is addressed to literature (Mannina *et al.* 2016a, 2016b; Mannina 2017; Mannina *et al.* 2017a, 2017b, 2018).

Dissolved and gaseous N₂O concentrations were measured in each reactor and in the permeate by using a gas chromatograph (Thermo Scientific™ TRACE GC) equipped with an electron capture detector (ECD).

Furthermore, the N₂O-N fluxes (gN₂O-N m⁻² h⁻¹) from all reactors were quantified by measuring the gas flow rates, Q_{GAS} (L min⁻¹) (Mannina *et al.* 2017a, 2017b).

Briefly, Q_{GAS} was evaluated indirectly, through the following expression (1):

$$Q_{gas} = v_{gas} \cdot A \quad (1)$$

where A represents the outlet section (m²) and v_{gas} (m s⁻¹) is the gas velocity, measured by using a TMA-21HW - Hot Wire anemometer. The gas flow rate is further converted in nitrous oxide flux by taking into account the N₂O concentration measured in the Q_{GAS}.

Gas samples were withdrawn by means of commercial syringes and transferred into glass vials (e.g. LABCO Exetainer, 738 model) where the vacuum was previously created. In order to guarantee the atmospheric pressure inside the vials, the ratio between the volume of the gas sample (inserted inside the vial) and the volume of the vial was no less than 1.25 (e.g. 15 mL of sample in a 12 mL vial). Three replicates were performed for each grab sample. The N₂O-N concentration was then calculated as the average value among the three replicates.

Dissolved gas sampling was conducted on the basis of the head space gas method derived from Kimochi *et al.* (1998). In detail, 70 mL of supernatant (after 5 min of centrifugation at 8,000 rpm) were sealed into 125 mL glass bottles. To prevent any biological reaction, 1 mL of 2N H₂SO₄ was added. After 24 h of gentle stirring, the bottles were left for 1 h without moving. Thereafter, the gas accumulated in the headspace of the bottles was collected similarly to the gas sampling procedure.

For each compartment, the evaluation of the N₂O-N emission factors, expressed as the percentage of N₂O-N emitted compared to the inlet nitrogen loading rates, was conducted by means of the following Equation (2), derived by Tsuneda *et al.* (2005):

$$EF_{N_2O} = \frac{N_2O - N_{Gas}/HRT_{h,s} + N_2O - N_{Dissolved}/HRT}{TN_{IN}/HRT} \quad (2)$$

where EF_{N₂O} is the emission factor (EF), N₂O-NGas [mg N₂O-N L⁻¹] is the nitrous dioxide in the gaseous phase, N₂O-NDissolved [mg N₂O-N L⁻¹] is the nitrous dioxide in the liquid phase, TN_{IN} [mg TN L⁻¹] is the pilot plant influent total nitrogen concentration, HRT [h] is the hydraulic retention time of the investigated pilot plant while HRT_{h,s} [h] represents the headspace retention time of the analysed tank (e.g. the HRT_{h,s} of the aerobic reactor corresponds to

the head space volume of the aerobic reactor divided for the air flow rate evaluated in accordance to Equation (1)).

RESULTS AND DISCUSSION

By varying the experimental layout, as noticeable from Figure 1, an intensive campaign aimed at evaluating the nitrous oxide production has been carried out over almost two years. Such effort has been done in order to create a dataset of information useful to provide insights to better understand the nitrous oxide production and emission mechanisms. It is worth noticing that the extreme variability of N_2O required such a long investigation period; as an example, in Figure 2 the N_2O gaseous and dissolved concentration measured in the anoxic and aerobic reactors of the aforementioned pilot plants are depicted.

In detail, headspace data are representative of the N_2O concentration confined between the liquid surface and the funnel shape cover of the reactors, while the dissolved concentration data are representative of the N_2O present in the liquid bulk of each reactor. It is important to highlight that data depicted in Figure 2 are representative of the reactors, aerobic and anoxic, where the core part of the nitrogen transformation process occur. Data collected over almost two years underline the huge variability of N_2O concentration measured; the nitrous oxide concentrations ranged within seven orders of magnitude (from $10^{-1} \mu\text{g } N_2O\text{-N } L^{-1}$ up to $10^5 \mu\text{g } N_2O\text{-N } L^{-1}$).

Such extreme variability in N_2O concentrations also resulted in a wide range of EF measured during the experimentation. In Figure 3, the average value of emission factors measured for each experimental layout are depicted with the standard deviation.

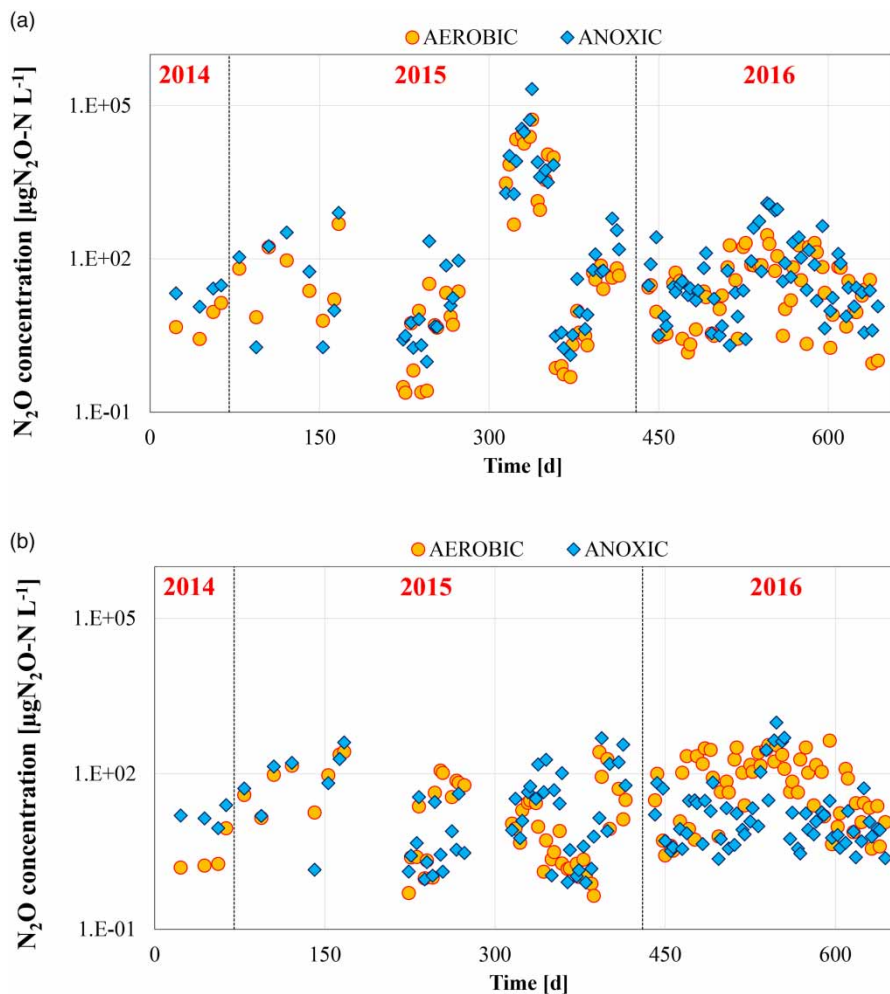


Figure 2 | Nitrous oxide concentration measured in the head space (a) and in the liquid bulk (b) of aerobic and anoxic reactors over the experimental campaign.

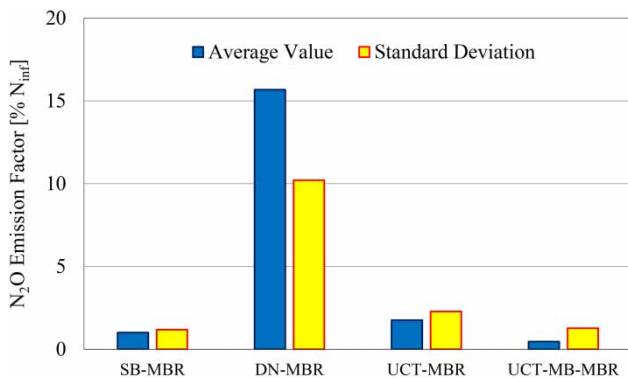


Figure 3 | Nitrous oxide average emission factor measured for each experimental layout. The bars report minimum and maximum value for each configuration.

Data depicted in Figure 3 highlight the influence exerted by the specific process scheme on the nitrous oxide emission. In detail, the DN-MBR process showed the highest EF (16% of influent nitrogen on average) as well as the highest standard deviation (close to 10%). It is worth noting that the influent wastewater composition also played a significant role in increasing the N₂O emission. The DN-MBR scheme treated an influent wastewater composed also by salt and diesel fuel (Mannina *et al.* 2016b). The co-presence of salt and hydrocarbon represented a disturbance factor that, affecting the metabolic activity of biomass, increased the N₂O production and thus the emission. The role played by the salinity is also noticeable during the operation as SB-MBR configuration. The stepwise salinity increase resulted in a moderate EF (mean EF measured during SB-MBR period resulted equal to 1% of influent nitrogen). The mean dissolved concentration of nitrous oxide during SB-MBR operation ranged from 1.5 µg N₂O-N L⁻¹ to 38.5 µg N₂O-N L⁻¹. A similar concentration was measured in the head space during the DN-MBR configuration. During the SB-MBR period, the maximum nitrous oxide concentrations, dissolved and in the head space, were measured constantly in the anoxic reactor. Such an occurrence highlights that the main N₂O production pathway during SB-MBR configuration was the anoxic heterotrophic denitrification.

With regard to the UCT-MBR and IFAS-UCT-MBR configuration, the scarcity of carbon availability imposed during the lowest values of C/N ratio resulted in an increase of N₂O emission likely due to a limitation of denitrification process and to the inhibition of the complete nitrification (Mannina *et al.* 2017b, 2018). A significant NO₂ accumulation (till to the average value of 30 mg L⁻¹) in the aerobic reactor occurred in the IFAS-UCT-MBR configuration at C/N equal to 2, resulting in incomplete nitrification due to nitrite oxidizing bacteria inhibition (Mannina *et al.* 2017c). Conversely, a

slight accumulation of NO₂ occurred during C/N equal to 5 for the UCT-MBR configuration (1.2 mg L⁻¹) (Mannina *et al.* 2016c).

To summarize, the configuration that yielded the lowest EF was the UCT-MB-MBR that was featured by a mean emission equal to 0.5% of influent nitrogen. Actually, the operational condition influenced the emission also during this period. As an example, when an SRT = 30 d was imposed to the pilot plant, the mean EF resulted equal to 7.57%.

In order to also describe the role played by each reactor in contributing to the total emission, in Figure 4 is depicted a comparison of mean EF assessed for each reactor during UCT-MBR and IFAS-UCT-MBR configuration. Data in Figure 4 highlight the strong reduction in EF during the IFAS-UCT-MBR layout.

Such a result is likely due to an improvement in biological performances exerted by the co presence of both suspended and attached biomass. The biofilm presence improved the nitrogen removal efficiency thus leading to a lower N₂O emission. It is worth noticing that the highest emissions were measured, during operation of both layout, in the aerated reactors (aerobic reactor and MBR compartment), thus confirming the significant role played by the aeration devices in enhancing the N₂O stripping favouring the emission.

In order to better discuss the influence played by the operational conditions as well as by the layout configurations on the nitrous oxide production, in Figure 5 a comparison of mean N₂O dissolved concentration measured in the biological reactors during C/N period of UCT-MBR and IFAS-UCT-MBR layout is depicted.

Data reported in Figure 5 allow noticing the increase in N₂O dissolved concentration measured due to the C/N

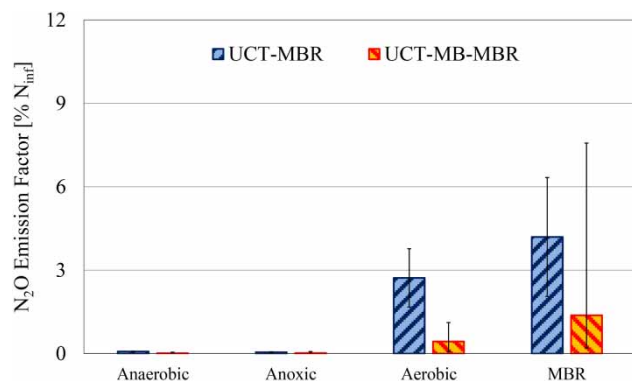


Figure 4 | Comparison of mean EF measured in each biological reactor during the UCT-MBR and IFAS-UCT-MBR layout.

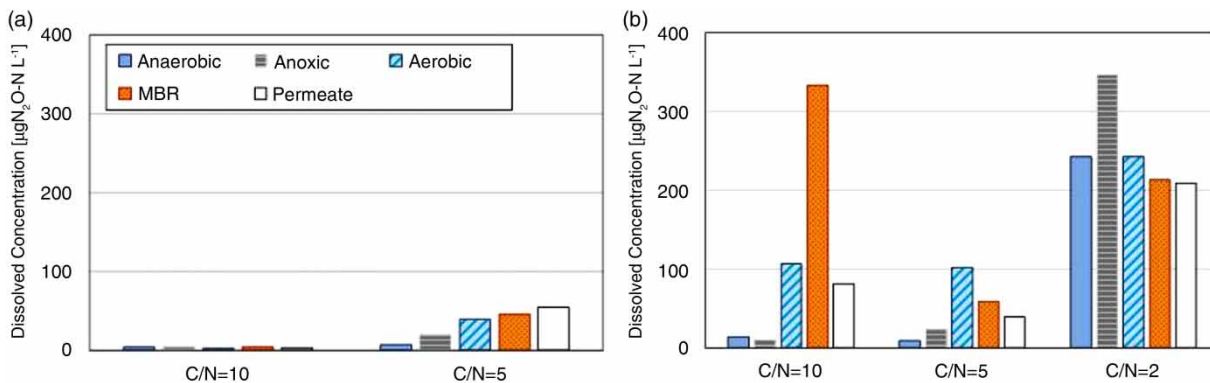


Figure 5 | Comparison of mean N_2O dissolved concentration measured in the biological reactors during C/N period of UCT-MBR (a) and IFAS-UCT-MBR (b) layout.

reduction. Such a result that was achieved by using real domestic wastewater is consistent with previous findings (Itokawa *et al.* 2001; Alinsafi *et al.* 2008; Kampschreur *et al.* 2009; Lu & Chandran 2010). In detail during the UCT-MBR layout (Figure 5(a)), the decrease of C/N fed to the pilot plant resulted in a drastic increase of dissolved nitrous oxide concentration. As an example, the mean N_2O concentration measured in the permeate flow during C/N = 10 period was equal to $9.21 \mu\text{g } N_2O\text{-N } L^{-1}$. Conversely, when the carbon availability was reduced due to the lower C/N, the mean N_2O concentration measured in the permeate flow increased up to $95.85 \mu\text{g } N_2O\text{-N } L^{-1}$, thus 10 times higher than the preceding period.

Also for the IFAS-UCT-MBR configuration (Figure 5(b)), a high emission occurred at the low C/N ratio; however, it is worth noticing that, during the C/N = 2 period, the highest N_2O dissolved concentration was measured in the anoxic reactor. In detail, during C/N = 10 and C/N = 5 period, the maximum values of N_2O concentration were measured in the aerobic or in the MBR reactor. When the C/N = 2 was imposed, the absence of organic carbon available for denitrification led to a sharp increase of nitrous oxide production likely in the denitrification zone that reached the average concentration of $347 \mu\text{g } N_2O\text{-N } L^{-1}$.

The mean N_2O dissolved concentration measured in the anoxic reactor during C/N = 10 and C/N = 5 were equal to $9.47 \mu\text{g } N_2O\text{-N } L^{-1}$ and $21.45 \mu\text{g } N_2O\text{-N } L^{-1}$, respectively. Similar considerations can also be done by observing the N_2O concentration measured in the anaerobic reactor during the C/N = 2 period. Indeed, the mean N_2O dissolved concentration in the anaerobic increased up to $244.20 \mu\text{g } N_2O\text{-N } L^{-1}$ in the C/N = 2 period, thus more than 10 times higher than the other periods. These results are due to the absence of organic carbon available for the denitrification that resulted also in an increase of

nitrites recycled to the anaerobic reactor. As a consequence, during the C/N = 2 period, the anaerobic reactor resulted in being overloaded by nitrites, thus acting as an anoxic reactor and contributing to the high N_2O production.

CONCLUSIONS

In this study, the overall assessment of N_2O emissions from fully covered MBR pilot plants was performed. Different MBR configurations, operational conditions and influent features were investigated in view of better understanding the key factors mainly influencing the N_2O emission in MBRs.

The following conclusions can be drawn:

- The aerated reactors (including MBR) represent the main source in terms of N_2O emission for all the investigated configurations. Therefore, in the MBRs the aeration devices play a key role in enhancing the N_2O stripping favouring the emission.
- A strong variability of N_2O produced/emitted from each tank was observed.
- The highest absolute N_2O emission (16% of the influent nitrogen) was observed when industrial wastewater contaminated with salt and hydrocarbons were treated (in a DN-MBR configuration); therefore, particular attention has to be paid on gases produced from industrial WWTPs.
- Biofilm systems allow an improvement of the nitrogen removal efficiency thus leading to a lower N_2O emission.
- The influent C/N ratio has a key role in promoting/reducing the N_2O emission. In a biofilm system (IFAS-UCT-MBR), the reduction of the influent C/N

ratio (from 10 to 2) led to the doubling of the N₂O dissolved concentration of each tank.

ACKNOWLEDGEMENTS

This work forms part of a research project supported by a grant of the Italian Ministry of Education, University and research (MIUR) through the research project of national interest PRIN2012 (D.M. 28 dicembre 2012 n. 957/Ric – Prot. 2012PTZAMC) entitled ‘Energy consumption and Green House Gas (GHG) emissions in the wastewater treatment plants: a decision support system for planning and management – <http://ghgfromwwtp.unipa.it>’ – in which the first author of this paper is the Principal Investigator. Giorgio Mannina is Fulbright Research Fellow at Columbia University, New York, NY, USA.

REFERENCES

- Ahn, J., Kim, S., Park, H., Katehis, D., Pagilla, K. & Chandran, K. 2010 Spatial and temporal variability in atmospheric nitrous oxide generation and emission from full-scale biological nitrogen removal and non-BNR processes. *Water Environ. Res.* **82**, 2362–2372.
- Alinsafi, A., Adouani, N., Beline, F., Lendormi, T., Limousy, L. & Sire, O. 2008 Nitrite effect on nitrous oxide emission from denitrifying activated sludge. *Process Biochem.* **43**, 683–689.
- Chandran, K., Stein, L. Y., Klotz, M. G. & Van Loosdrecht, M. C. M. 2011 Nitrous oxide production by lithotrophic ammonia-oxidizing bacteria and implications for engineered nitrogen-removal systems. *Biochem. Soc. Trans.* **39** (6), 1832–1837.
- Di Trapani, D., Capodici, M., Cosenza, A., Di Bella, G., Mannina, G., Torregrossa, M. & Viviani, G. 2011a Evaluation of biomass activity and wastewater characterization in a UCT-MBR pilot plant by means of respirometric techniques. *Desalin.* **269**, 190–197.
- Di Trapani, D., Mannina, G., Torregrossa, M. & Viviani, G. 2011b Quantification of kinetic parameters for heterotrophic bacteria via respirometry in a hybrid reactor. *Water Sci. Technol.* **61** (7), 1757–1766.
- Ekama, G. A., Siebritz, I. P. & Marais, G. R. 1985 Considerations in the process design of nutrient removal activated sludge processes. *Water Sci. Technol.* **15** (3–4), 283–318.
- IPCC 2007 Changes in atmospheric constituents and in radiative forcing. In: *Climate Change 2007: The Physical Science Basis. Contribution of Working Group I to the Fourth Assessment Report of the Intergovernmental Panel on Climate Change* (S. Solomon, D. Qin, M. Manning, Z. Chen, M. Marquis, K. B. Averyt, M. Tignor & H. L. Miller, eds). Cambridge University Press, Cambridge, UK, pp. 114–143.
- Itokawa, H., Hanaki, K. & Matsuo, T. 2001 Nitrous oxide production in high-loading biological nitrogen removal process under low COD/N ratio condition. *Water Res.* **35** (3), 657–664.
- Kampschreur, M. J., Temmink, H., Kleerebezem, R., Jetten, M. S. M. & van Loosdrecht, M. C. M. 2009 Nitrous oxide emission during wastewater treatment. *Water Res.* **43**, 4093–4103.
- Kimochi, Y., Inamori, Y., Mizuochi, M., Xu, K.-Q. & Matsumura, M. 1998 Nitrogen removal and N₂O emission in a full-scale domestic wastewater treatment plant with intermittent aeration. *J. Ferment. Bioeng.* **86**, 202–206.
- Law, Y., Ye, L., Pan, Y. & Yuan, Z. 2012 Nitrous oxide emissions from wastewater treatment processes. *Philos. Trans. R. Soc. B Biol. Sci.* **367**, 1265–1277.
- Lu, H. & Chandran, K. 2010 Factors promoting emissions of nitrous oxide and nitric oxide from denitrifying sequencing batch reactors operated with methanol and ethanol as electron donors. *Biotechnol. Bioeng.* **106** (3), 390–398.
- Mannina, G. 2017 *Frontiers in Wastewater Treatment and Modelling-FICWTM 2017* (G. Mannina, ed.). Series Lecture Notes in Civil Engineering, Springer, Palermo, Italy.
- Mannina, G., Morici, C., Cosenza, A., Di Trapani, D. & Ødegaard, H. 2016a Greenhouse gases from sequential batch membrane bioreactors: a pilot plant case study. *Biochem. Eng. J.* **112**, 114–122.
- Mannina, G., Cosenza, A., Di Trapani, D., Laudicina, V. A., Morici, C. & Ødegaard, H. 2016b Nitrous oxide emissions in a membrane bioreactor treating saline wastewater contaminated by hydrocarbons. *Bioresour. Technol.* **219**, 289–297.
- Mannina, G., Capodici, M., Cosenza, A. & Di Trapani, D. 2016c Carbon and nutrient biological removal in a University of Cape Town membrane bioreactor: analysis of a pilot plant operated under two different C/N ratios. *Chemical Engineering Journal* **296**, 289–299.
- Mannina, G., Capodici, M., Cosenza, A., Di Trapani, D., Laudicina, V. A. & Ødegaard, H. 2017a Nitrous oxide from moving bed based integrated fixed film activated sludge membrane bioreactors. *Journal of Environmental Management* **187**, 96–102.
- Mannina, G., Capodici, M., Cosenza, A., Di Trapani, D. & van Loosdrecht, M. 2017b Nitrous oxide emission in a University of Cape Town membrane bioreactor: the effect of carbon to nitrogen ratio. *J. Clean. Prod.* **149**, 180–190.
- Mannina, G., Ekama, G. A., Capodici, M., Cosenza, A., Di Trapani, D. & Ødegaard, H. 2017c Moving bed membrane bioreactors for carbon and nutrient removal: the effect of C/N variation. *Biochemical Engineering Journal* **125**, 31–40.
- Mannina, G., Capodici, M., Cosenza, A., Di Trapani, D. & Ekama, G. A. 2018 The effect of the solids and hydraulic retention time on moving bed membrane bioreactor performance. *Journal of Cleaner Production* **170**, 1305–1315.
- Ni, B. & Yuan, Z. 2015 Recent advances in mathematical modeling of nitrous oxides emissions from wastewater treatment processes. *Water Res.* **87**, 336–346.
- Nuansawan, N., Boonnorat, J., Chiemchaisri, W. & Chiemchaisri, C. 2016 Effect of hydraulic retention time and sludge

- recirculation on greenhouse gas emission and related microbial communities in two stage membrane bioreactor treating solid waste leachate. *Bioresour. Technol.* **210**, 35–42.
- PRIN2012 2012 Energy consumption and GreenHouse Gas (GHG) emissions in the wastewater treatment plants: a decision support system for planning and management. <http://ghgfromwwtp.unipa.it>.
- Stenström, F., Tjus, K. & la Cour Jansen, J. 2014 Oxygen-induced dynamics of nitrous oxide in water and off-gas during the treatment of digester supernatant. *Water Sci. Technol.* **69** (1), 84–91.
- Stephenson, T., Judd, S. J., Jefferson, B. & Brindle, K. 2000 *Membrane Bioreactors for Wastewater Treatment*. IWA Publishing, London, UK.
- Tsuneda, S., Mikami, M. & Kimochi, Y. 2005 Effect of salinity on nitrous oxide emission in the biological nitrogen removal process for industrial wastewater. *J. Hazard Mater* **119**, 93–98.
- Wunderlin, P., Mohn, J., Joss, A., Emmenegger, L. & Siegrist, H. 2012 Mechanisms of N₂O production in biological wastewater treatment under nitrifying and denitrifying conditions. *Water Res.* **46**, 1027–1037.
- Yu, R. & Chandran, K. 2010 Strategies of nitrosomonas europaea 19718 to counter low dissolved oxygen and high nitrite concentrations. *BMC Microbiology* **10**, 70.
- Yu, R., Kampschreur, M. J., Van Loosdrecht, M. C. M. & Chandran, K. 2010 Mechanisms and specific directionality of autotrophic nitrous oxide and nitric oxide generation during transient anoxia. *Environ. Sci. Technol.* **44** (4), 1313–1319.
- Yu, R., Perez-Garcia, O., Lu, H. & Chandran, K. 2018 Nitrosomonas europaea adaptation to anoxic-oxic cycling: insights from transcription analysis, proteomics and metabolic network modeling. *Sci. Total Environ.* **615**, 1566–1573.

First received 13 December 2017; accepted in revised form 10 August 2018. Available online 22 August 2018